STUDIA UBB CHEMIA, LXI, 2, 2016 (p. 137-154)
(RECOMMENDED CITATION)

# PROMOTED ALUMINA SUPPORTED Ni CATALYST FOR ETHANOL STEAM REFORMING

**MONICA DAN[a], MARIA MIHET, MIHAELA DIANA LAZAR[a*], LIANA MARIA MURESAN[b*]**

**ABSTRACT.** The catalytic behavior of Ni/γ-$Al_2O_3$ catalyst modified with Cu, Ag, and Au was investigated in the process of ethanol steam reforming. The catalysts were prepared by co-impregnation and were characterized by specific surface area determination ($S_{BET}$), Inductively Coupled Plasma Mass Spectrometry (ICP-MS), X-ray diffraction (XRD), temperature programmed reduction (TPR), temperature programmed desorption (TPD) The data obtained from the experiments revealed that even at temperature as low as 350°C the ethanol is converted entirely, showing high selectivity for $H_2$ and $CH_4$.The activity of the Ni/γ-$Al_2O_3$ is only slightly increased by the addition of the supplementary metals. Nevertheless, the addition of metals to Ni/γ-$Al_2O_3$ has a positive effect in diminishing the quantity of $CO_2$ produced in the reaction. The promoted alumina Ni catalysts present a higher stability in some experimental conditions.

***Keywords:*** *Ethanol steam reforming, Ni-catalysts, hydrogen production*

## INTRODUCTION

Hydrogen is involved in many chemical and petrochemical processes, being considered as a promising clean energy vector [1,2]. Due to the increasing concern regarding environmental issues, an alternative to the fossil fuels it's demanded by the global society. New renewable energy sources which include $H_2$ are investigated by the research community. $H_2$ is mainly produced in industry from steam reforming of natural gas, a process who contributes to the greenhouse effect [3].

[a] *National Institute for Research and Development of Isotopic and Molecular Technologies, 67-103 Donath Street, 400293 Cluj-Napoca, Romania*
[*] *Corresponding authors: diana.lazar@itim-cj.ro, limur@chem.ubbcluj.ro*
[b] *Babeş-Bolyai University, Faculty of Chemistry and Chemical Engineering, 11 Arany Janos str., RO-400028, Cluj-Napoca, Romania*

Therefore, renewable sources like biomass for the production of hydrogen attract increased interest [4,5]. Among various bio-derived feedstocks, ethanol has the advantage of high hydrogen content, low toxicity and easiness in storing and handling. The ethanol can be transformed in hydrogen in conditions of relative low temperature and pressure (through steam reforming).

The reaction scheme of the ethanol steam reforming (ESR) is composed of a main reaction:

$$C_2H_5OH + 3H_2O \rightarrow 2CO_2 + 6H_2 \quad (1)$$

and a series of other parallel reactions, the most common of them being: [6–8]

- ethanol decomposition $C_2H_5OH \rightarrow CH_4 + CO + H_2$ (2)
- ethanol dehydrogenation $C_2H_5OH \rightarrow CH_3CHO + H_2$ (3)
- ethanol dehydration $C_2H_5OH \rightarrow C_2H_4 + H_2O$ (4)

The acetaldehyde can further decompose to form $CH_4$ and CO or can undergo steam reforming:

$$CH_3CHO \rightarrow CH_4 + CO \quad (5)$$
$$CH_3CHO + H_2O \rightarrow 2CO + 3H_2 \quad (6)$$

The CO formed in (eq.2) and (eq.5) can further be oxidized to $CO_2$ through water gas shift (eq.7) or to form carbon through Boudouard reaction (eq.8):

$$CO + H_2O \rightarrow CO_2 + H_2 \quad (7)$$
$$2CO \leftrightarrow C + CO_2 \quad (8)$$

Also, the ethylene can polymerize and form coke [9]:

$$nC_2H_4 \rightarrow \text{polymers} \rightarrow C \quad (9)$$

It is relatively obvious that the reactions involved in ethanol steam reforming process are many and complex and their relative occurrence depend on the nature of the catalytic material and of the reaction conditions.

The catalyst is crucial in order to obtain a good hydrogen production. According to the literature, different types of catalyst were tested in the process of ethanol steam reforming: oxides [10,11], noble and non noble metals [12–15]. Noble metals such as Ru, Rh, Pt, and Pd on various supports are well known for their high catalytic activity and stability. The main drawback of these catalysts is their high cost and relatively low availability.

Nickel and cobalt are mostly used as catalysts in ESR process [16,17] presenting good catalytic activity and low cost. The values recorded for ethanol conversion and for hydrogen selectivity in the process of ESR

using supported Ni catalyst are relatively high. However, there is a major drawback for this type of catalyst, mainly the poor stability in time, the catalyst deactivation occurring due to carbon deposition. The promotion of the supported Ni catalysts with other elements can improve the catalysts stability but also the catalytic activity. There are studies that suggest that carbon deposition on Ni catalysts for steam reforming of hydrocarbons can be strongly suppressed by adding promoters such as Ag or Au [18,19].

Catalysts based on copper are most interesting for ESR process. The catalytic properties of this type of catalyst depend strongly on the interaction of the metal with the support [20]. Copper is shown to act as a promoter on the catalytic activity and stability of the catalyst [21][22]. Alumina is one of the most used supports in ESR process having a high thermal stability.

The aim of this paper was to study the catalytic performances of alumina supported Ni catalysts promoted with Cu, Ag and Au at low temperature and high S/C ratio in the process of steam reforming of ethanol. The effect of addition of supplementary metals was studied in terms of structural modification, ethanol conversion, hydrogen yield, and catalyst stability.

## RESULTS AND DISCUSSION

### Catalyst characterization

Determined by ICP-MS method, the nickel content of the prepared catalysts is similar for Ni/Al and Ni-Au/Al with a value of 6.8 wt% and lower for Ni-Ag/Al and Ni-Cu/Al (Table 1).

The recorded $N_2$ adsorption-desorption isotherms for all studied catalysts show a type IV isotherm usually associated with a mesoporous structure [23]. The total surface area ($S_{tot}$), pore volume and pore size are not significantly affected by the addition of the supplementary metal (Table 1). The pore's radius varies between 20Å and 40Å for all the catalysts.

**Table 1.** Structural characteristics of Ni catalysts

| Catalyst | $S_{tot}$ ($m^2/g$) | $S_{Ni}$ ($m^2/g$) | $C_{Ni}$ (%) | $C_{metal}$ (%) | $D_{Ni\text{-}XRD}$ (nm) |
|---|---|---|---|---|---|
| Ni/Al | 102 | 2.4 | 6.8 | - | 10.0 |
| Ni-Ag/Al | 105 | 1.2 | 6.0 | 0.9 | 7.2 |
| Ni-Au/Al | 109 | 2.2 | 6.8 | 1.0 | 8.7 |
| Ni-Cu/Al | 104 | 1.3 | 6.1 | 0.8 | 5.9 |

From Ni chemisorption measurements we were able to calculate the surface of catalytic active area (Table 1). The values of the Ni surface area for Ni/Al and Ni-Au/Al are similar and are lower for Ni-Ag/Al and Ni-Cu/Al.

TPR experiments were performed on the calcinated catalysts precursors in order to evaluate the type and strength of interaction between $NiO_x$ species and the support in correlation with the addition of the second metal. In order to clearly identify the reduction peaks, the TPR recorded profile was subjected to a mathematical analysis using a Gaussian function. Thus, for Ni/Al, three major peaks situated at 673°C, 735°C and 802°C were identified (Figure 1). It is generally accepted that the lower temperature peaks are associated with the presence of $NiO_x$ particles with weak interaction to the support, while the high temperature peaks correspond to $NiO_x$ species in close contact with the support [24]. The peaks situated below 673°C prove the existence of $NiO_x$ species with low and medium interaction to the alumina support. The peaks situated above the 700°C are in general associated with the reduction of highly dispersed $NiAlO_4$.

The shape of the recorded TPR profile of the bimetallic catalysts is different from the TPR profile corresponding to Ni/Al. The addition of the noble metals (Ag, Au) to Ni/Al has the effect of lowering the main reduction peak from 735°C for NI/Al to 534°C for Ni-Ag/Al and 557°C for Ni-Au/Al. Also low intensity peaks are observed with values situated between 140°C-300°C associated to $NiO_x$ species with low interaction with the support.

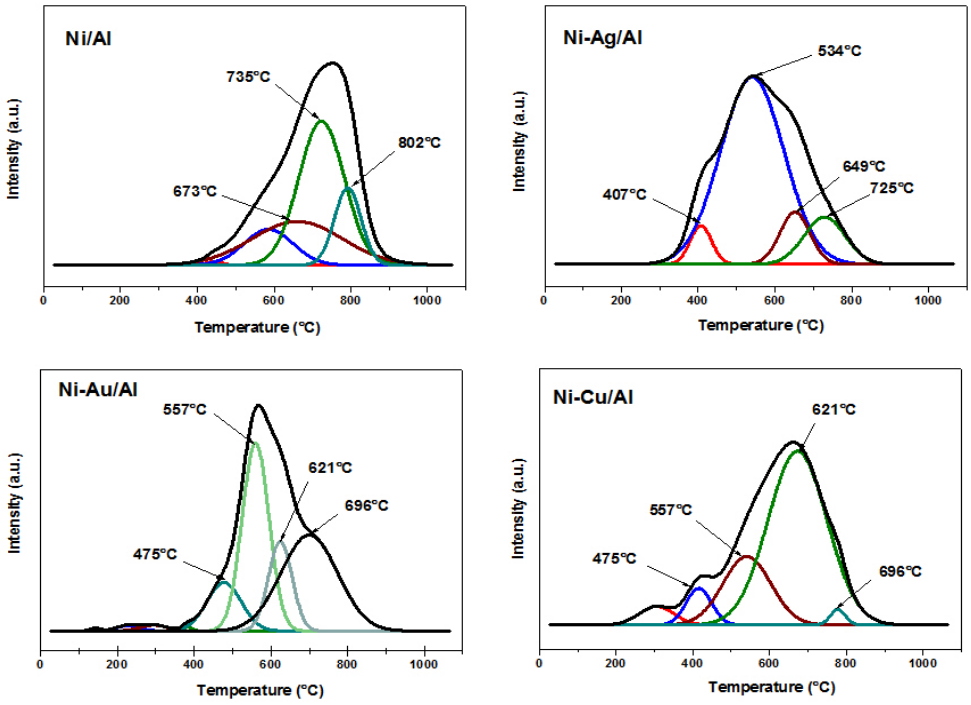


**Figure 1.** TPR profile of alumina supported nickel catalysts

The addition of copper to Ni/Al has a similar effect by lowering the temperature of the main reduction peak to 672°C from 735°C. Also, around 430°C a supplementary peak is present which could correspond to the reduction of CuO or to a NiO species as well. The peaks situated at 320°C correspond entirely to the reduction of CuO species [25]. In conclusion the addition of all three studied metals to $Ni/Al_2O_3$ decreases the strength of $NiO_x$ interaction with the support increasing thus the reducibility of catalyst precursor.

From the XRD patterns of the prepared Ni catalysts, it was possible to determine the support crystallinity and the size of Ni crystallites (Figure 2). For all the catalysts the presence of the Ni corresponding diffraction peaks were observed at 44.5°, 51.8° and 76.5°. The Bragg reflexions situated at 37.3° and 43.3° and associated with NiO are not present, suggesting thus the presence of Ni only in the metallic state [26]. The presence of metallic Au, Ag and Cu could not be confirmed, probably due to the low quantity of the metal. The spectral lines associated with the presence of CuO at 20°, 33° also could not be confirmed. From XRD patterns the nickel crystallites size was calculated for all samples using Scherrer's equation (Table 1). The addition of all three studied metals decreases the Ni crystallites size in the following order: Ni-Cu/Al < Ni-Ag/Al < Ni-Au/Al < Ni/Al. The strongest effect was observed for Cu which produced the decrease of Ni crystallites size at almost half, inducing thus a much higher dispersion of active metal on the catalyst surface. For Ni-Cu/Al and Ni-Ag/Al the decrease of Ni nanoparticles is not correlated with variation of Ni surface area. Normally, a higher Ni dispersion is associated with higher metal surface area, which is not the case here. The only explanation would be that for these two catalysts a fraction of additional metal is deposited on the top of Ni nanoparticles. For Ni-Au/Al the addition of Au does not significant influence the catalyst structure.

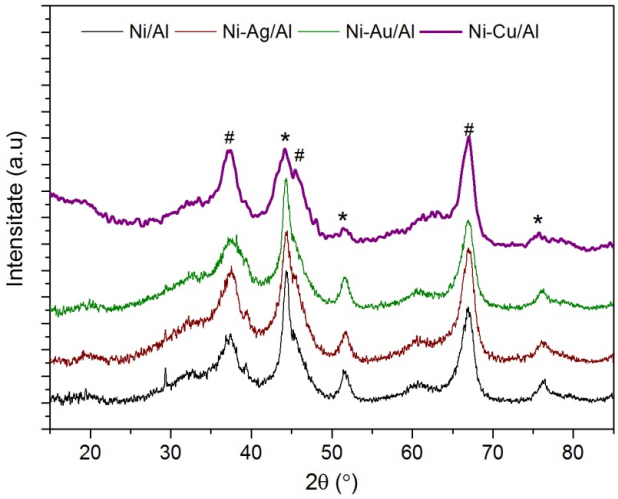


**Figure 2.** XRD pattern of the fresh prepared supported Ni catalyst: *- Ni, #-Al

$H_2$-TPD investigations were performed in order to obtain information regarding the type and strength of catalytic active sites for hydrogen chemisorption and activation and also on the influence that the additional metals might have on the nature of the catalytic active sites. The recorded profile shows in general two domain of hydrogen desorption peaks: one situated at lower temperature denoted as type I peaks, and one situated at higher temperature denoted as type II peaks. Type I peaks correspond to hydrogen desorbed form Ni nanoparticles and is in direct correlation with the number of Ni catalytic active sites [27, 28]. The hydrogen which is originally located on subsurface layers and/or the spillover hydrogen is usually associated with type II peaks [24].

The recorded TPD profile of the investigated catalytic material presents an asymmetric shape for all the alumina supported Ni catalyst. In order to distinguish between these two types of peaks the TPD profile were deconvoluted using a Gaussian type function (Figure 3).

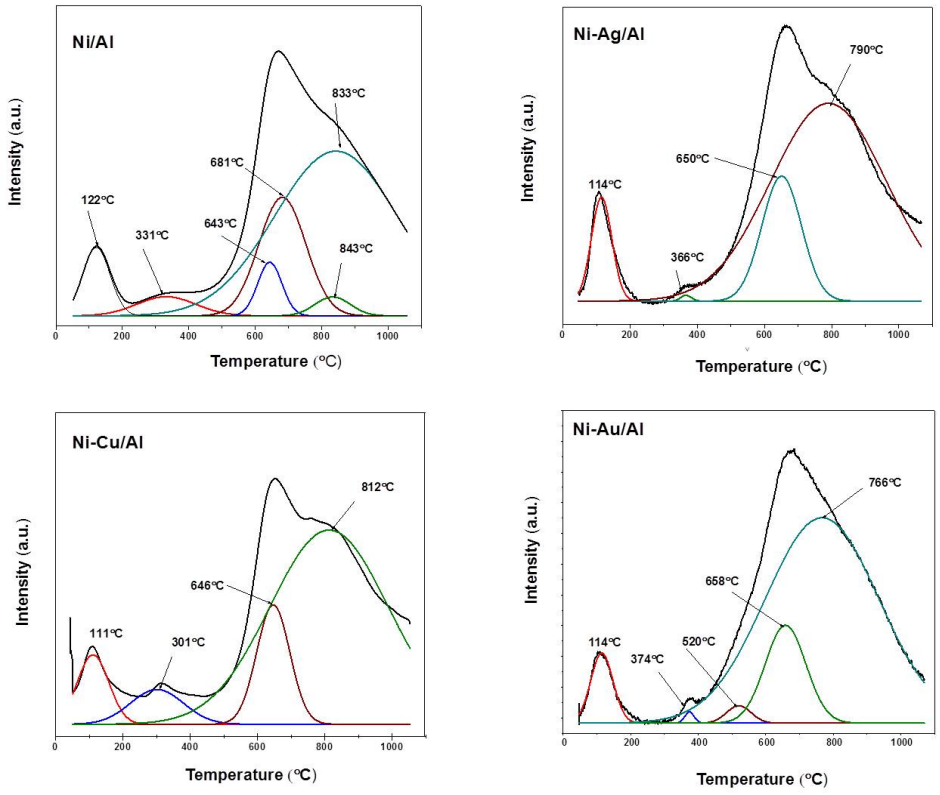


**Figure 3.** $H_2$-TPD profile of alumina supported Ni catalysts

From the deconvolution of the desorption curves it has been observed the presence of both type I and type II peaks. For all the investigated catalysts the distinction between the type I (below 500°C) and type II (above 500°C) desorption regions is very clear. For all the catalysts the identified peaks are mainly type II which suggest that all of the investigated catalyst have a high capacity to store hydrogen subsurface and/or on the support. For Ni/Al and Ni-Cu/Al two types of peaks were distinguished in region I: type Ia situated at temperature values <200°C, and types Ib with values 200°C<T<500°C, which indicates the presence of two different Ni catalytic active sites with different strength of H-Ni bonds. For Ni-Ag/Al and Ni-Au/Al the intensity of the Ib type peak is very low, demonstrating the prevalence of only one type of Ni catalytic sites.

The conclusion of the catalysts characterization section is that the addition of the supplementary metals (Ag, Au and Cu) to the alumina supported Ni catalyst leads to better reducibility of the catalyst precursor and better dispersion of Ni on the catalyst surface. The addition of Cu, Ag and Au does not change the mesoporous structure of the alumina supported catalysts and has a only a small influence on the type and strength of catalytic sites for hydrogen chemisorption.

### Catalyst activity and selectivity

The Ni catalysts supported on alumina were tested in ethanol steam reforming at low temperature (150°C - 350°C) and high water-ethanol ratio (EtOH - $H_2O$ = 1:30 molar ratio). The low temperature used in this study tries to improve the energy costs of the hydrogen production process. Another important aspect that was taken into consideration is the possibility of improving the water gas shift reaction and diminishing the concentration of CO, by working at low temperature (eq. 7) [29]. Also, we have chosen such a high water-ethanol ratio in order to try to reduce the carbon deposition on the catalyst surface of the studied catalyst.

Each catalyst was tested for 24 h at each temperature with 133 ml/min flow of carrier gas. The liquid (ethanol-water mixture) feed rate was varied between 0.1-0.6 ml/min.

The ethanol conversion function of temperature and liquid feed is presented in (Figure 4). At the lowest studied temperature - 150°C, regardless of the liquid feed, the ethanol conversion is around or less than 50%. At this temperature the addition of the supplementary metal to Ni/Al does not seem to have a significant positive effect on the ethanol conversion except for 0.3 ml/min feed rate.

At the highest temperature (350°C) for 0.1 ml/min and 0.3 ml/min liquid feed rate the maximum conversion is attained for all studied catalysts. For 0.6 ml/min liquid feed rate a decrease in ethanol conversion is recorded regardless of the imposed working temperature. In these working conditions a positive effect of metal addition upon ethanol conversion was attained, especially in the case of Ag and Cu. At lower reagents flow the 100% conversion observed for all catalysts impede the observation of any possible influence of additional metal to the catalyst performance.

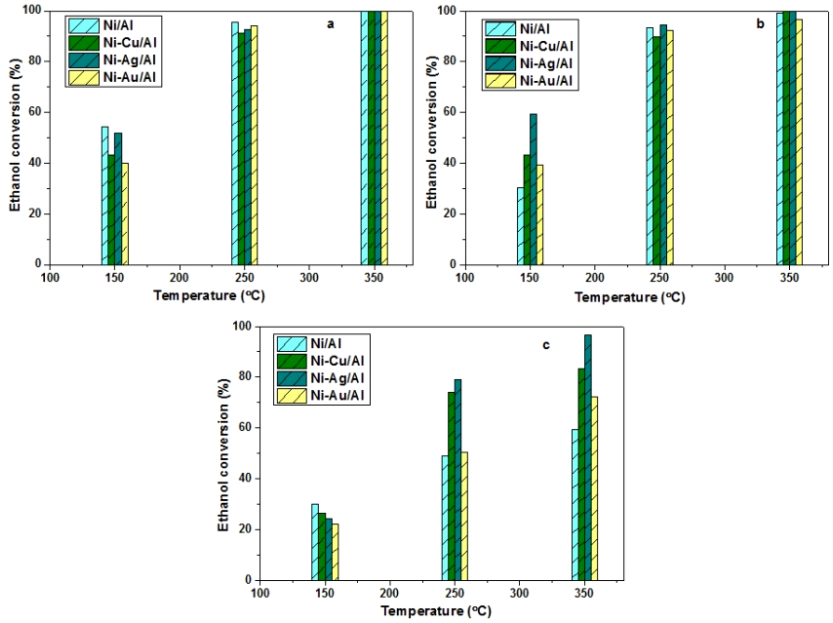


**Figure 4.** Ethanol conversion with temperature and liquid feed rate in ethanol steam reforming reaction: a-0.1ml/min; b-0.3ml/min; c-0.6ml/min

The TOF number (turn over frequency) was calculated in order to estimate the influence of metals on the intrinsic catalytic activity of Ni active sites. The TOF results (Table 2) at 150°C and 0.1 ml/min feed rate suggest a similar catalytic activity for Ni/Al and Ni-Ag/Al and a lower one for Ni-Au/Al. Although the TOF number for Ni-Cu/Al is higher than the one obtained for Ni/Al this is not reflected in a higher ethanol conversion. One possible explanation for this is that Ni/Al has a higher surface area, higher Ni dispersion which leads to a higher number of Ni catalytic active sites and therefore to a better overall catalytic activity.

At 150°C and 0.3 ml/min liquid feed rate it can be observed a direct correlation between high values of TOF number and high values for ethanol conversion for Ni-Ag/Al and Ni-Cu/Al, compared to the values recorded for Ni/Al.

**Table 2.** Catalytic parameters for all tested catalysts in ethanol steam reforming

| Catalyst | TOF x $10^{-2}$ ($s^{-1}$) | | | | | | N x $10^{18}$ (at/g cat) |
|---|---|---|---|---|---|---|---|
| | Liquid flow ml/min | | | | | | |
| | 0.1 | | 0.3 | | 0.6 | | |
| | 150°C | 350°C | 150°C | 350°C | 150°C | 350°C | |
| Ni/Al | 2.5 | 4.6 | 4.2 | 13 | 8.3 | 16 | 37 |
| Ni-Cu/Al | 3.7 | 8.6 | 11 | 25 | 13.6 | 42 | 20 |
| Ni-Ag/Al | 4.8 | 9.3 | 16 | 28 | 13.4 | 53 | 19 |
| Ni-Au/Al | 2 | 5.1 | 5.9 | 14 | 6.7 | 22 | 34 |

TOF-turnover frequency; N-number of catalytic active sites per g catalyst

The results obtained at 350°C and 0.6 ml/min feed rate, revealed high values for TOF for all the bimetallic catalyst compared to Ni/Al. This is reflected also in the conversion of ethanol which is higher for all the tested catalysts with additional metal.

The liquid products are removed from the mixture through condensation at the reactor exit. Besides water, the liquid mixture also contains unreacted ethanol (depending on ethanol conversion) and traces of acetaldehyde and acetone. The gaseous phase is dried by passing it through a silica trap and then analyzed on line. The identified products are: $H_2$, CO, $CH_4$, and $CO_2$. No traces of other light alkynes or alkenes were identified, although these compounds are mentioned in other studies [30]. At low experimental temperature $H_2$ is the main compound in the gaseous mixture regardless of liquid feed rate and of the investigated catalyst (Figure 5).

The distribution of products in the gaseous mixture is modified due to the various reactions that are favoured by increasing the temperature. At 350°C we observe that hydrogen selectivity at a given value of liquid feed is not significantly influenced by the addition of the supplementary metals. By increasing the reagents flow the relative concentration of $H_2$ in the exhausted gases increase with almost 20% reaching around 70% values (Figure 6). This is only partially due to the decrease of relative concentration of methane, which would imply an increase of catalyst selectivity for hydrogen production, and mainly to the decrease of carbon oxides concentrations. At 0.1 ml/min liquid feed and 350°C the values of the $CO_2$ selectivity are drastically decreased by the addition of the supplementary metals to Ni/Al. Important concentrations of CO were recorded especially for Ni-Au/Al catalyst. By raising the liquid feed rate to 0.6 ml/min the relative concentration of $CO_2$ is lower, as mentioned before, but the same trend of decreasing of the $CO_2$ selectivity is observed for promoted catalysts (Figure 6).

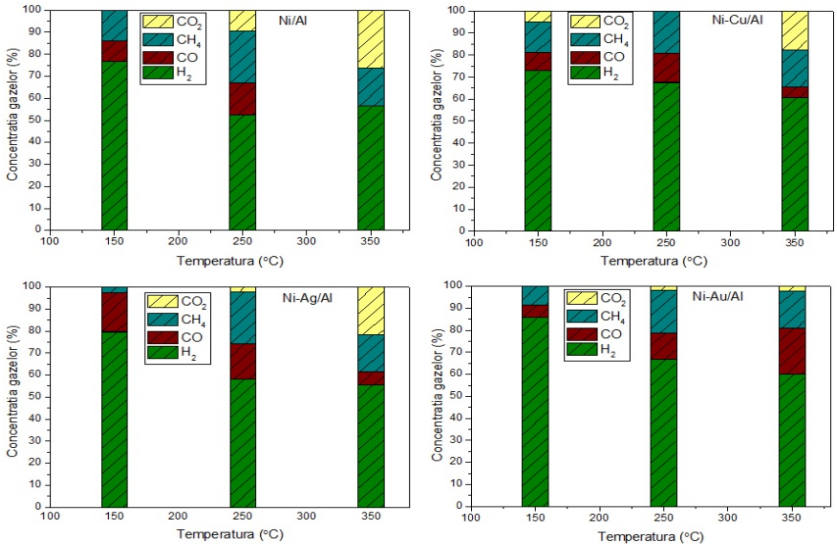


**Figure 5**. Composition of effluent gases (mol %) in ethanol steam reforming at 0.1 ml/min liquid feed rate

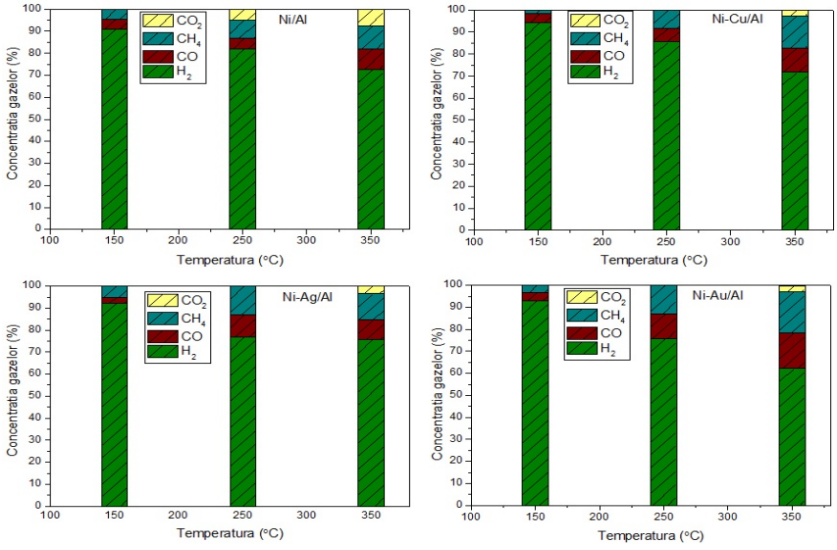


**Figure 6.** Composition of effluent gases (mol %) in ethanol steam reforming at 0.6 ml/min liquid feed rate

The hydrogen yield is an important catalytic parameter (calculated according to (eq. (10)) which characterizes the catalyst efficiency to obtained hydrogen from the raw material in ESR reaction (Figure 7). At the lowest

working temperature the obtained values are low due to low conversion of ethanol. Increasing the temperature to maximum (350°C) we obtained higher values for this parameter. Its value is situated around 30% being not significantly influenced by the metal addition or the reagents flow.

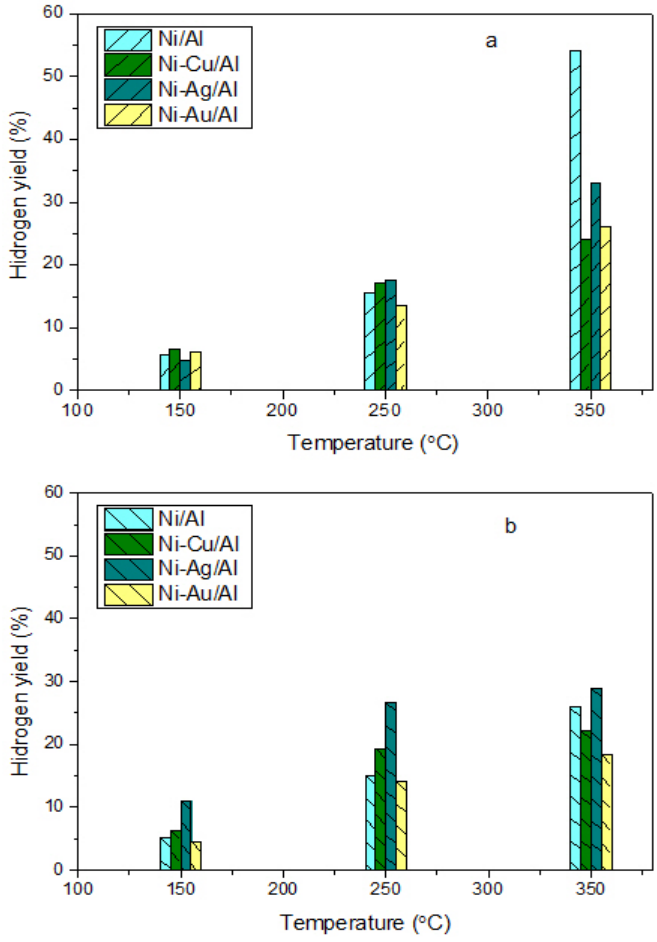


**Figure 7.** The variation of hydrogen yield with temperature and liquid feed rate in ethanol steam reforming reaction: a - 0.1 ml/min; b - 0.6 ml/min

The stability of the catalyst was evaluated during 24h on stream by measuring on line the ethanol conversion. It was observed at lower experimental temperature and lower feed rate a decrease in ethanol conversion higher than the one recorded for ESR experiments at higher temperature.

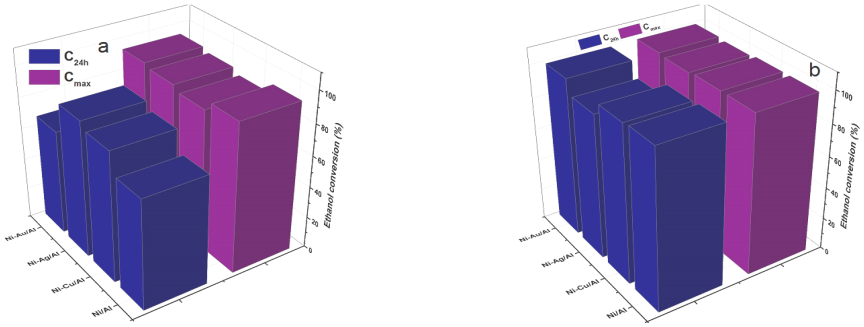


**Figure 8.** Catalyst stability for alumina supported Ni catalysts in ESR reaction at 0.1 ml/min liquid feed rate a-250°C; b-350°C; $C_{max}$-maximum ethanol conversion, $C_{24h}$- ethanol conversion after 24h

The addition of metals (Au, Ag, and Cu) to Ni/Al seems to have a positive effect by diminishing the catalyst deactivation in most of the tested experimental conditions. Thus, the promoted catalysts tested at the 0.1 ml/min flow rate at 250°C and 350°C present lower deactivation, except Ni-Au/Al at 250°C for which a drop of almost 30% from the initial value of ethanol conversion is recorded (Figure 8a).

With the increase of liquid feed rate to 0.6 ml/min at 250°C a deactivation of all the catalysts was observed: Ni-Au/Al deactivates almost completely and Ni/Al at ≈50% from the maximum values of ethanol conversion. Contrarily, for Ni-Ag/Al and Ni-Cu/Al a beneficial effect of additional metal is clearly observed (Figure 9a). For the same liquid feed rate and 350°C the recorded deactivation for all the tested catalyst is even more pronounced, Ni-Au/Al being the catalyst for which the recorded deactivation is the highest (Figure 9). It can be concluded that the stability of all catalysts at 0.6 ml/min liquid flow and 350°C is very poor despite their good initial catalytic activity.

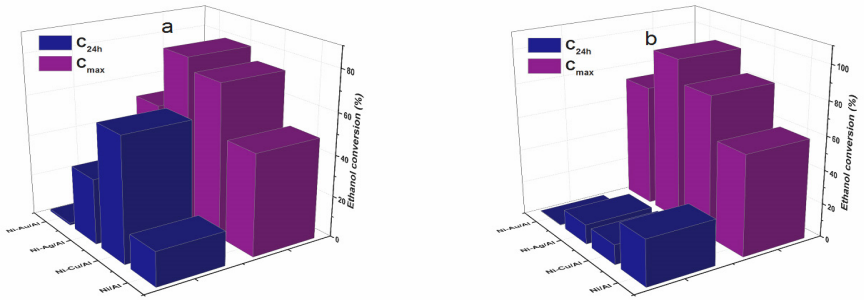


**Figure 9.** Catalyst stability for alumina supported Ni catalysts in ESR reaction at 0.6 ml/min liquid feed rate a-250°C; b-350°C; $C_{max}$-maximum ethanol conversion, $C_{24h}$- ethanol conversion after 24h

The deactivation of the catalyst in ESR reaction is mainly due to the formation of carbon and its deposition on the catalyst surface [31]. In order to investigate the catalysts deactivation for 0.6 ml/min liquid flow, XRD techniques were used.

The XRD analysis of the used catalyst revealed that the lines that should be attributed to Cu, Ag and Au do not appear in the spectra, due to the low amount of the metal deposited on the support. The recorded spectra did not contain any peak in the area of 2θ = 26.5° [33] that could be assigned to graphitic carbon. Besides the lines attributed to $Al_2O_3$ and Ni, the presence of NiO at 2θ= 43°, was also revealed for Ni/Al and the Cu and Ag promoted catalysts (Figure 10). NiO is not active for ESR and is a cause of catalysts deactivation. In this case, the high flow rate and high water: ethanol ratio provide an oxidizing environment at 350° which lead to Ni oxidation to NiO with subsequent loose of catalytic activity. The addition of another metal does not strongly influence this phenomenon. At 250° the addition of Cu and Ag interfere in the process and reduce the catalyst deactivation (Figure 9a).

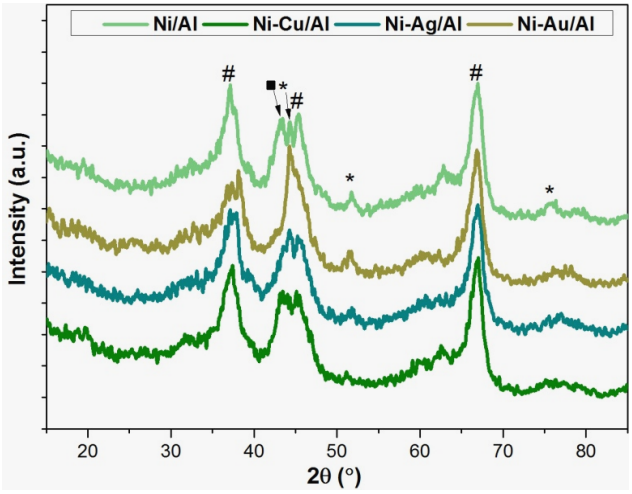


**Figure 10.** XRD spectra of the alumina-Ni supported catalysts used in the ESR reaction at 350°C and 0.6 ml/min liquid feed flow

## CONCLUSIONS

An investigation of group Ib belonging metals promoted on alumina supported Ni catalysts (Ni/Al, Ni-Ag/Al, Ni-Au/Al, Ni-Cu/Al) used in the process of ethanol steam reforming at low temperature and high water:ethanol ratio was carried out. The catalysts were prepared by co-impregnation and characterized by ICP-MS, XRD, TPR and $H_2$-TPD.

The addition of the supplementary metal to Ni/Al improves the reducibility of the catalyst precursor and the Ni dispersion, but does not change the mesoporous structure of the catalyst. The maximum ethanol conversion is obtained at temperature of 350°C and 0.1 ml/min and 0.3 ml/min of liquid feed rate. Better catalytic activity was recorded for the bimetallic catalyst at 350°C and 0.6 ml/min compared to Ni/Al, but the stability is very poor for all tested catalysts on these experimental conditions.

The reaction products mixture contains high proportion of hydrogen and low proportion of methane alongside the carbon oxides; the values of $CO_2$ selectivity are lower for the bimetallic catalysts compared to those for Ni/Al. The highest hydrogen yield was recorded for Ni/Al at 350°C and 0.1 ml/min liquid feed rate. The addition of metals (Ag, Au, Cu) to Ni/Al proves to have a positive effect by diminishing the catalyst deactivation only in some experimental conditions.

## EXPERIMENTAL SECTION

### Catalysts preparation

The $Ni/Al_2O_3$ (denoted Ni/Al) catalyst was prepared by wet impregnation of γ-alumina (Merck, Germany, $S_{tot}$= 135 $m^2/g$) with an aqueous solution of $Ni(NO_3)_2 \cdot 6H_2O$. The co-impregnation method was used to prepare the promoted alumina supported nickel catalysts. Thus $Ni\text{-}Cu/Al_2O_3$ (denoted Ni-Cu/Al), $Ni\text{-}Ag/Al_2O_3$ (denoted Ni-Ag/Al), $Ni\text{-}Au/Al_2O_3$ (denoted Ni-Au/Al) were prepared by impregnation of γ-alumina with a mixture of aqueous solution of $Ni(NO_3)_2 \cdot 6H_2O + Cu(NO_3)_2 \cdot 6H_2O$, $Ni(NO_3)_2 \cdot 6H_2O + AgNO_3$, $Ni(NO_3)_2 \cdot 6H_2O + HAuCl_4$.

The impregnated catalysts samples were dried at room temperature overnight, calcinated in Ar at 550°C for 4h followed by reduction with $H_2$ at 550°C for another 4h. All reagents unless other specified were purchased from Alfa Aeser, Germany and used with no further purification.

### Catalyst characterization

Metal content was determined by ICP-MS analysis using an ELAN DCR-e instrument (Perkin-Elmer, USA). The metals were removed from the support by treating 0.1 g catalyst sample with 5 ml of concentrated $HNO_3$ for nickel, copper and silver containing samples. In order to determine the gold content, the catalyst sample was treated with 5 ml of "*aqua-regia*".

Adsorption desorption isotherms obtained using a Sorptomatic 1900 (Thermo Electron Corporation, USA) instrument were used to determine the total surface area ($S_{tot}$), pore volume ($V_p$) and pore radius ($r_p$).

X-ray powder diffraction (XRD) spectra were recorded using a Brucker $D_8$ advanced diffractometer with $CuK_{\alpha 1}$ radiation source, operated voltage 40 kV and 40 mA current. The diffraction patterns were recorded in the range $20° < 2\theta < 85°$ with a step size of 0.01°/s. The size of Ni crystallites was determined using Scherrer's equation.

The active surface area of the catalysts was measured by $H_2$ chemisorption in conventional volumetric equipment. The sample (≈ 2.5 g) was reduced overnight at 350°C in hydrogen flow and degassed at the same temperature until a final pressure lower than $10^{-5}$ torr was attained. Adsorption of hydrogen was carried out at room temperature. The metallic surface area was calculated assuming a stoichiometry of 1:1 H to Ni atom and that each nickel atom occupies 6.5 $Å^2$.

Using as equipment TPRO 1100 (Thermo Scientific, USA) it was possible to record the profile obtained from $H_2$ temperature programmed reduction (TPR) and $H_2$ temperature programmed desorption (TPD) experiments of every prepared catalyst. For TPR experiments 0.35 g of calcinated catalyst precursor was placed in the reactor with Ar for 30 min and then heated from room temperature to 1100°C, with a rate of 10°C/min with a 20 ml/min ($H_2$ +Ar) mixture (10 vol% $H_2$).

For TPD experiments, about 0.35 g of catalyst was activated in the same mixture ($H_2$+ Ar) at 550°C for 4 h and then cooled down to 50°C in Ar (20 ml/min). Hydrogen chemisorption was performed at 50°C in ($H_2$+Ar) mixture for 1h followed by cleaning in Ar for 30min. Hydrogen desorption were made by heating the catalyst sample in Ar (20 ml/min) from 50°C to 1100°C, with a temperature rate of 10°C/min.

**Catalyst activity testing**

The catalytic activity of the prepared catalyst was evaluated in the process of ethanol steam reforming. The experimental setup is described in detail (Figure 11). The experiments were performed at ambient pressure in a stainless steel (i.d. 9 mm) fixed bed reactor placed in a temperature controlled oven. The carrier gas (Ar) is controlled by a mass flow controller and the liquid mixture (ethanol-water) is introduced in the reaction system through LC-6A (Shimadzu, Japan) pump. At the reactor outlet, the liquid phase is removed from the outcoming mixture through condensation. The effluent gas is further dried by passing it through silica gel. Furthermore the gas is analyzed on-line using a gas chromatograph (Sferocarb column, 2m, 80-100 mesh and Ar as carrier gas at 120°C) equipped with a TCD detector.

The catalyst (1g) is mixed with alumina support (1g) with the same granulation (100-200 μm) and placed in the reactor. Prior to catalytic activity test, the catalyst is reduced in $H_2$ at 350°C for 3h. The temperature

range of the experiments is set between 150°C and 350°C at atmospheric pressure. The $H_2O$: EtOH volumetric ratio was 9:1 (10 vol% solution of EtOH in water) which gives an $H_2O$: EtOH molar ratio of 30:1.

Ethanol conversion was calculated using the following formula:

$$C_{EtOH} = \frac{[EtOH]_{in} - [EtOH]_{out}}{[EtOH]_{in}} x100 \quad (10)$$

where $[EtOH]_{in}$ and $[EtOH]_{out}$ are ethanol molar concentrations in the initial solution and in the outlet condensed liquid, respectively.

Hydrogen yield was calculated according to the formula:

$$H_2 \text{ yield} = \frac{\text{moles } H_2 \text{ produced}}{6 \text{ x (moles EtOH converted)}} \text{ x } 100 \quad (11)$$

The identified compounds in the gas mixture are expressed in mol %, taking into consideration only the reaction products and not the carrier gas.

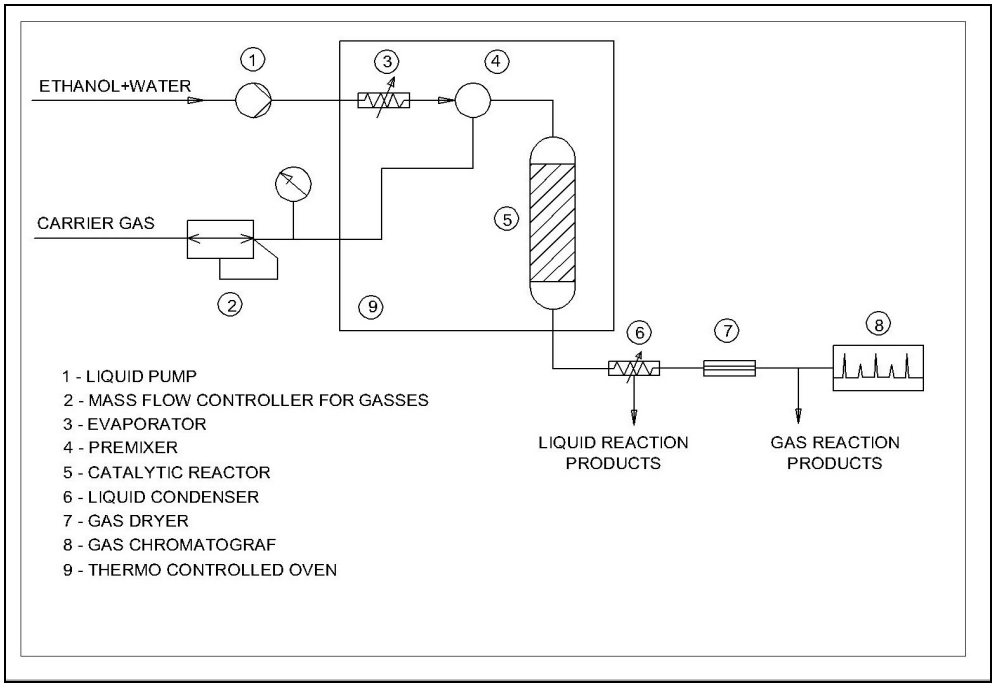


**Figure 11.** The schematics of the experimental setup for the ethanol steam reforming process

## ACKNOWLEDGMENTS

This work was supported by a grant of the Romanian National Agency for Scientific Research, Project Number PN-II-PT-PCCA-2011-3.2-0452

## REFERENCES

1. A. Züttel, A. Remhof, A. Borgschulte, O.Friedrichs, *Philosophical Transactions Series A Mathematical, physical, and engineering sciences,* **2010**, 368, 3329–3342.
2. C. Pirez, M. Capron, H. Jobic, F. Dumeignil, L. Jalowiecki-Duhamel, *Angewandte Chemie International Edition,* **2011**, 50, 10193–10197.
3. L. He, J.M.S. Parra, E.A. Blekkan, D.Chen, *Energy Environmental Science,* **2010**, 3, 1046–1056.
4. P.R. Piscina, N.Homs , *Chemical Society Reviews,* **2008**,37, 2459–2467.
5. D.M. Alonso, S.G. Wettstein, J.A. Dumesic, *Chemical Society Review*, **2012**, 41, 8075–8098.
6. W. Xu, Z. Liu, A.C. Johnston-Peck, S.D. Senanayake, G. Zhou, D. Stacchiola et al., *American Chemical Society Catalysis,* **2013**, 3, 975–984.
7. G. A. Deluga, J.R. Salge, L.D. Schmidt, X.E. Verykios, *Science* **2004**, 303, 993–997.
8. A. Therdthianwong, T. Sakulkoakiet, S. Therdthianwong, *Science Asia*, **2001**, 27,193–198.
9. A.N. Fatsikostas, X.E. Verykios, *Journal of Catalysis*, **2004**, 225, 439–452.
10. M. Skotak, Z. Karpinski, W. Juszczyk, J. Pielaszek, L. Kepinski, D. Kazachkin et al., *Journal of Catalysis,* **2004**, 227, 11–25.
11. M.C. Sánchez-Sánchez, R.M. Navarro, J.L.G Fierro, *International Journal of Hydrogen Energy,* **2007**, 32, 1462–1471.
12. P.Y. Sheng, H.Idriss, *Journal of Vacuum Science Technology A*, **2004**, 22, 1652-1658.
13. J. Raskó, A. Hancz, A. Erdőhelyi, *Applied Catalysis A General*, **2004**, 269, 13–25.
14. Z. Wang, C. Wang, S. Chen, Y. Liu, *International Journal of Hydrogen Energy,* **2014**, 39, 5644–5652.
15. R. Buitrago-Sierra, J. Ruiz-Martínez, J.C. Serrano-Ruiz, F. Rodríguez-Reinoso, A. Sepúlveda-Escribano, *Journal of Colloids and Interface Science*, **2012**, 383, 148–154.
16. S. Li, M. Li, C. Zhang, S. Wang, X. Ma, J. Gong, *International Journa of Hydrogen Energy,* **2012**, 37, 2940–2949.
17. R. Padilla, M. Benito, L. Rodríguez, A. Serrano, G. Muñoz, L.Daza, *Internatioanl Journal of Hydrogen Energy*, **2010**, 35, 8921–8928.
18. H.S. Bengaard, J.K. Nørskov, J. Sehested, B.S. Clausen, L.P. Nielsen, A.M. Molenbroek, et al., *Journal of. Catalysis*, **2002**, 209, 365–384.
19. N.V. Parizotto, K.O. Rocha, S. Damyanova, F.B. Passos, D. Zanchet, C.M.P. Marques, et al., *Applied Catalysis A General*, **2007**, 330, 12–22.
20. A. Kubacka, M. Fernández-García, A. Martínez-Arias, *Applied Catalysis A General.,* **2016**, in press, doi:10.1016/j.apcata.2016.01.027
21. C. Ratnasamy, J.P. Wagner, *Catalysis Reviews,* **2009**, 51, 325–440.

22. F. Wang, Y. Li, W. Cai, E. Zhan, X. Mu, W. Shen, *Catalysis Today* **2009**,146, 31–36.
23. S.J. Gregg. Adsorption, Surface area and Porosity, *Academic Press*, **1982**.
24. S. Velu, S.K. Gangwal, Solid State Ionics **2006**,177, 803–811.
25. H. Wang, R.T.K Baker, *The Journal Physical Chemistry B,* **2004**, 20273–20277.
26. Y. Matsumura, T. Nakamori, *Applied Catalysis A General,* **2004**, 258,107–114.
27. A.G. Boudjahem, S. Monteverdi, M. Mercy, M.M. Bettahar, *Journal of Catalysis,* **2004**, 221, 325–334.
28. Y. Cesteros, P. Salagre, F. Medina, J. Sueiras, *Applied Catalysis B Environmetal,* **2000**, 25, 213–227.
29. L. García, Compendium of Hydrogen Energy, **2015**.
30. G. Rabenstein, V. Hacker, *Journal of Power Sources,* **2008**,185,1293–1304.
31. L.V. Mattos, G. Jacobs, B.H. Davis, F.B. Noronha., *Chemical Reviews,* **2012**, 112, 4094–4123.
32. Z.L. Zhang, Verykios XE., *Catalysis Today,* **1994**, 21, 589–595.
33. A. Tanksale, J.N. Beltramini, G.M. Lu., *Renewable Sustainable Energy Reviews.,* **2010**, 14, 166–182.